Original Article

Evaluation of Initial Stress Distribution and Displacement Pattern of Craniofacial Structures with 3 Different Rapid Maxillary Expansion Appliance Models: A 3-dimensional Finite Element Analysis

Merve Sucu[1] ⬤, Berza Yilmaz[2] ⬤, Sabri İlhan Ramoğlu[3] ⬤

[1]Specialist in Orthodontics, Private practice, Istanbul, Turkey
[2]Department of Orthodontics, Faculty of Dentistry, Bezmialem Vakif University, Istanbul, Turkey
[3]Department of Orthodontics, Faculty of Dentistry, Altinbas University, Istanbul, Turkey

I8

Main points:
- All the appliances showed similar stress distributions.
- The maximum posterior expansion was achieved with the Hyrax appliance.
- The maximum anterior expansion was observed with the double-hinged appliance.
- Inferior maxillary displacement was the greatest with the Hyrax appliance.
- Anterior maxillary displacement was the greatest with the double-hinged appliance.

ABSTRACT

Objective: This study aimed to describe the displacement of anatomical structures and the stress distributions caused by the Hyrax, fan-type, and double-hinged expansion screws via the 3-dimensional (3D) finite element method (FEM).

Methods: The 3D FEM was based on the computed tomography data of a 12-year-old patient with a constricted maxilla. The Hyrax model included 1,800,981 tetrahedral elements with 2,758,217 nodes. The fan-type model included 1,787,558 tetrahedral elements with 2,737,358 nodes. The double-hinged model included 1,777,080 tetrahedral elements with 2,722,771 nodes. The von Mises stress distributions after 0.2 mm of expansion and displacement patterns after 5 mm of expansion were evaluated.

Results: The highest stress accumulation was observed in the sutura zygomatico maxillaris area with all 3 appliances. An increase in stress was noted at the pterygomaxillary fissure, the medial and lateral pterygoid process of the sphenoid bone, and the nasal areas. The wedge-shaped skeletal opening was observed with all 3 appliances. In the transverse plane, maximum posterior expansion was achieved with the Hyrax appliance, whereas the maximum anterior expansion was observed with the double-hinged appliance. The maxilla moved inferiorly and anteriorly with all the 3 appliances. The greatest inferior displacement of the maxilla was recorded with the Hyrax appliance, whereas anterior maxillary displacement was the greatest with the double-hinged appliance.

Conclusion: All the appliances showed similar stress distributions. The use of double-hinged screw caused a slight anterior displacement of point A. The fan-type and double-hinged appliances were shown to be more effective on anterior maxillary constriction, whereas the Hyrax appliance might be chosen for resolving maxillary posterior constriction.

Keywords: Finite Element Method, rapid maxillary expansion, transverse maxillary deficiency

INTRODUCTION

Rapid maxillary expansion (RME) is often needed to correct transverse discrepancies. RME is also used to correct the axial inclinations of the posterior teeth before functional jaw orthopedic or orthognathic surgery to mobilize the circummaxillary sutures, to reduce nasal resistance, and to broaden the smile (1).

Turk J Orthod 2021; 34(1): 18-25

Sucu et al. FEM Analysis of Three Different RME Appliances

The positional changes of the skeletal and dental structures after RME have been evaluated and documented in previous studies (2-4). Some authors have reported that the anatomical resistance areas are the dentoalveolar complex, midpalatal suture, zygomatico maxillary buttress, and circummaxillary sutures (4, 5). Isaacson (1964) and Wertz (1970) (2, 6) have stated that the resistance occurring during RME is caused by the neighboring tissues, such as zygomatic and sphenoid bones, and not the suture itself.
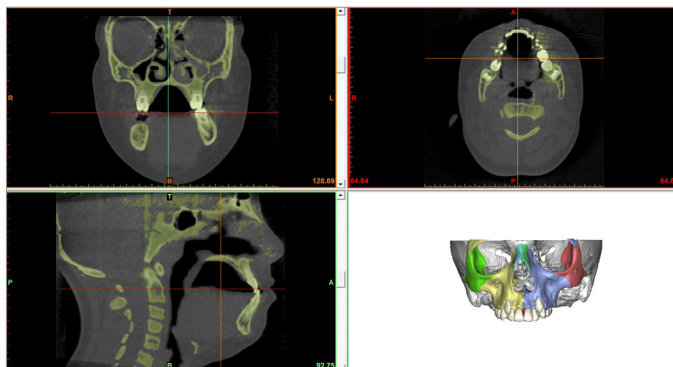
In recent years, the finite element method (FEM) has been proven to be a great research method to solve various biomechanical problems in orthodontics (7, 8). The possibility of simulating different clinical conditions without subjecting the patients to possible harmful adverse effects is one of the most important advantages of this method (9).

For anterior constriction, 2 different screw designs, the fan-type (10, 11) and the double-hinged type (12,13), were introduced instead of the conventional expansion Hyrax screw, which has been reported to expand the anterior part compared with the posterior part of the maxilla (4, 14). Multiple FEM studies have analyzed the effects of RME on the craniofacial complex and dentition; however, the effects of the fan-type and double-hinged expansion screws have not been evaluated with FEM yet (7-9).

This study aimed to analyze the stress concentration areas and displacement of the bony units with 3 different RME appliances on the same patient-based 3-dimensional (3D) FEM.

METHODS

The digital imaging and communications in medicine data were imported into the Mimics version 10.01 software (Materialise, Leuven, Belgium), and the bone tissue was calibrated (15). A computer-aided model was constructed based on the dental volumetric tomography scan of a 12-year-old male patient presenting with maxillary constriction. The cone-beam computed tomography image was taken with an Iluma Imtec Imaging machine (3M, Ardmore, OK, USA [X-ray tube, 120 kV; X-ray tube current, 1-4 mA; scanning time, 40 seconds maximum and 7.8 seconds minimum; field of view, 14.2x21.1 cm; voxel size, 0.0936 mm; greyscale, 14 bit]) with the patient sitting in an upright posi-

tion. The model containing only the nasomaxillary complex and the cranial bones was obtained by subtracting the mandibular and vertebral masks from the main mask (Figure 1).

Data of the models of the bony structures, teeth, and periodontium were exported to Geomagic Design X (Rock Hill, USA) and SOLIDWORKS 2016 software (SOLIDWORKS Corp, Waltham, Massachusetts, USA). Surface meshes were created; unwanted parts, such as overlaps, irregularities, roughness, and holes on the surface mesh structure, were arranged; and solid models were created for finite element analysis.

Figure 1. The digital imaging and communications in medicine images on Mimics software
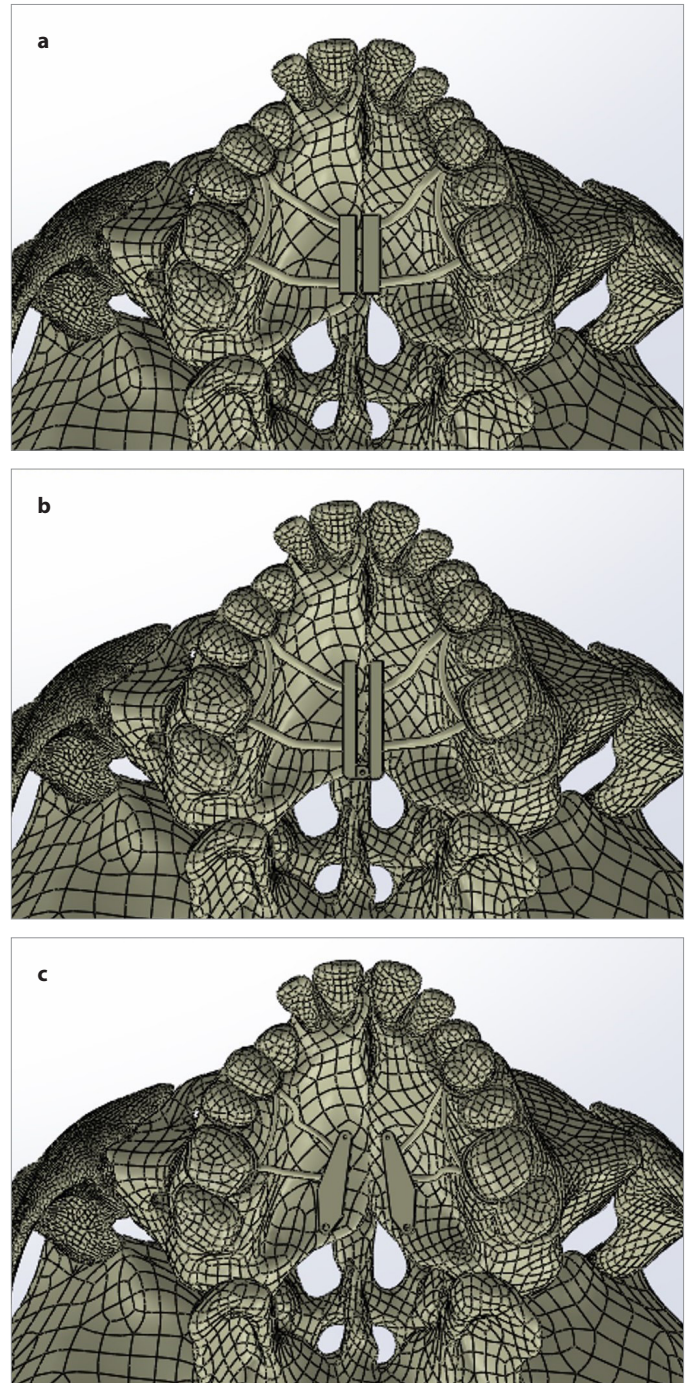
Figure 2. a-c. Modeling of the Hyrax appliance (a), modeling of the fan-type appliance (b), modeling of the double-hinged appliance (c)

Hyrax (Leone, Florence, Italy), fan-type (Leone, Florence, Italy), and double-hinged expanders (Bestdent, Kaoshiung, Taiwan) were modeled using SOLIDWORKS 2016. The screws were positioned parallel to the midpalatal suture, as close to the palate as possible (Figure 2a-2c).

ANSYS version 17.0 (Canonsburg, PA, USA) was used for the finite element analysis. The resulting volumetric Hyrax model included 1,800,981 tetrahedral elements with 2,758,217 nodes; the fan-type model included 1,787,558 tetrahedral elements with 2,737,358 nodes; And the double-hinged model included 1,777,080 tetrahedral elements with 2,722,771 nodes. Each element had a tetrahedral shape and included 10 nodes (Figure 3).

The teeth, cortical and cancellous bones, sutures, periodontal ligament, and stainless steel were considered to be homogenous and isotropic. The material properties, which were determined from the data of the previous studies, are shown in Table 1 (16-21).

Nodes along the foramen magnum were determined as the boundary condition, and all the displacements were restricted to this area (Figure 4) (7, 8, 22). The 2 parts of the maxilla were separated so that they could move with expansion forces laterally with respect to the vertical plane of symmetry (7).

This study was approved by the ethics committee of the Bezmialem Vakıf university clinical research (15.09.2015-17/18). Using the data extracted from the archival dental volumetric tomog-
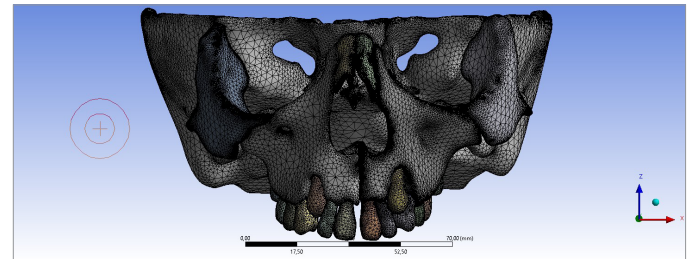

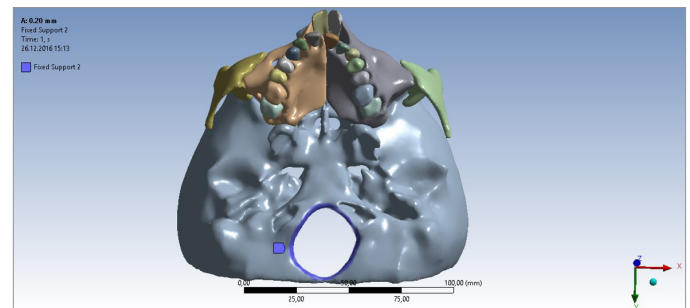**Figure 3.** Finite element analysis solid model

Table 1. Young's modulus and Poisson's ratio used in this study

	Young's modulus (MPa)		Poisson's ratio
Compact bone	13,700	1	0.3
Cancellous bone	1,370	2	0.3
Suture	10	3	0.49
Tooth	20,290	4	0.3
PDL	0.68	5	0.49
Stainless steel	210,000		0.3
PDL: fibrous connective tissue that surrounds the root and connects to the alveolar bone			

Figure 4. Boundary conditions

Table 2. Displacement of various skeletal structures (mm)

Skeletal structures	Hyrax				Fan-type				Double-hinged		
	X	Y	Z		X	Y	Z		X	Y	Z
Internasal suture	0.07	-0.26	-1.3	5.1	0.05	0	-0.61	5.2	-0.01	0.03	-0.47
Frontonasal suture	0.05	-0.36	-1.19	5.3	0.05	-0.07	-0.52	5.4	0.06	-0.01	-0.34
Frontomaxillary suture	0.02	-0.27	-1.05	5.5	0	-0.03	-0.43	5.6	-0.04	0.02	-0.24
Nasomaxillary suture	-0.03	-0.23	-1.15	5.7	-0.07	-0.02	-0.45	5.8	-0.16	-0.01	-0.28
Frontal process	-0.14	-0.2	-0.97	5.9	-0.21	-0.03	-0.3	5.10	-0.31	-0.03	-0.08
Zygomatico maxillary suture	-0.58	0.2	-0.19	5.11	-0.54	0.28	0.21	5.12	-0.73	0.15	0.47
Inferior orbital rim	-0.5	0.12	-0.23	5.13	-0.5	0.22	0.18	5.14	-0.71	0.22	0.46
Infraorbital foramen	-0.64	0.1	-0.5	5.15	-0.62	0.13	-0.01	5.16	-0.82	0.04	0.22
Zygomatic process	-0.76	0.34	-0.18	5.17	-0.67	0.29	0.17	5.18	-0.87	0.21	0.4
Lateral nasal cavity wall	-0.75	-0.13	-1.04	5.19	-0.79	-0.1	-0.33	5.20	-1.08	-0.22	-0.13
ANS	-1.24	-0.2	-1.34	5.21	-1.13	-0.24	-0.59	5.22	-1.44	-0.44	-0.39
Point A	-1.38	-0.1	-1.28	5.23	-1.23	-0.18	-0.53	5.24	-1.54	-0.38	-0.32
PNS	-0.63	-0.25	-1.11	5.25	-0.55	-0.26	-0.49	5.26	-0.73	-0.47	-0.37
Pterygomaxillary fissure	-0.38	0.25	-0.11	5.27	-0.31	0.16	0.15	5.28	-0.46	0.08	0.3
Medial pterygoid (inferior)	-0.47	0.17	-0.26	5.29	-0.36	0.05	0.01	5.30	-0.5	-0.08	0.09
Medial pterygoid (superior)	-0.05	-0.05	-0.21	5.31	-0.06	-0.05	0		-0.1	-0.01	0.02
Lateral pterygoid (inferior)	-0.43	0.23	-0.07	5.32	-0.32	0.12	0.14	5.33	-0.46	0.02	0.25
Lateral pterygoid (superior)	-0.16	0.11	-0.08		-0.16	0.09	0.12		-0.22	0.04	0.19
ANS: Anterior point on maxillary bone; PNS: Posterior point of palatine bone											

Table 3. Displacement of various dentoalveolar and dental structures (mm)

Dentoalveolar and dental structures	Hyrax				Fan-type				Double-hinged		
	X	Y	Z		X	Y	Z		X	Y	Z
Apical region of incisor	-1.5	0	-1.21	6	-1.32	-0.14	-0.48	7	-1.75	-0.4	-0.34
Apical region of canine	-1.13	0.04	-0.91	8	-1	-0.02	-0.26	9	-1.29	-0.17	-0.04
Apical region of premolar	-1.3	0.33	-0.56	10	-1.07	0.19	-0.04	11	-1.39	0.04	0.19
Apical region of molars	-0.96	0.41	-0.23	12	-0.78	0.29	0.14	13	-1.02	0.18	0.35
Incisal edge of incisor	-2.01	0.16	-1.33	14	-1.8	-0.08	-0.54	15	-2.21	-0.41	-0.31
Palatinal cusp tip of canine	-1.67	0.36	-0.82	16	-1.31	0.1	-0.16	17	-1.72	-0.12	-0.04
Palatinal cusp tip of molar	-1.55	0.37	-0.53		-0.84	0.26	-0.03		-1.35	0	0.11

Table 4. Von Mises stress distribution of various skeletal structures (MPa)

Skeletal structures	Von Mises (Mpa)		
	Hyrax	Fan-type	Double-hinged
Internasal suture	1.12	1.72	2.23
Frontonasal suture	1.27	1.57	1.59
Frontomaxillary suture	2.63	2.17	2.36
Nasomaxillary suture	2.51	2.07	2.16
Frontal process	1.55	0.53	0.58
Zygomatico maxillary suture	6.39	4.32	4.46
Inferior orbital rim	0.07	0.01	0.33
Infraorbital foramen	1.24	0.74	1.88
Zygomatic process	1.97	0.92	2.13
Lateral nasal cavity wall	1.2	0.87	1.22
ANS	0	0	0
Point A	0.01	0	0
PNS	0.04	0.01	0.05
Pterygomaxillary fissure	4.86	3.66	4.26
Medial pterygoid (inferior)	0.18	0.05	0.11
Medial pterygoid (superior)	3.19	1.49	2.54
Lateral pterygoid (inferior)	0.18	0.1	0.12
Lateral pterygoid (superior)	2.52	1.39	2

ANS: Anterior point on maxillary bone; PNS: Posterior point of palatine bone

Table 5. Von Mises stress distribution of various dentoalveolar and dental structures

Dentoalveolar and dental structures	Von Mises (Mpa)		
	Hyrax	Fan-type	Double-hinged
Apical region of incisor	0	0	0
Apical region of canine	0.45	0.63	0.71
Apical region of premolar	0.29	0.37	0.44
Apical region of molar	0.88	0.23	0.53
Incisal edge of incisor	0	0	0
Palatinal cusp tip of canine	0.06	0.11	0.13
Palatinal cusp tip of molar	0.26	0.19	0.19

ian of the patient previously signed an informed consent form stating that his archival data could be used for scientific purposes.

RESULTS

The 3D coordinates were recorded for various craniofacial structures before and after the screw activation in all 3 dimensions (X-axis-positive value: lateral movement, X-axis-negative value: medial movement, Y-axis-positive value: posterior movement, Y-axis-negative value: anterior movement, Z-axis-positive value: inferior movement, Z-axis-negative value: superior movement). Positive changes indicated lateral, posterior, and inferior displacements. The von Mises stress distribution was recorded after 0.2 mm of expansion, and the displacement of the structures was evaluated after 5 mm of expansion (Tables 2-5).

In this study, the von Mises stress distributions were investigated after the initial 0.2 mm of activation as in previous studies (28). In the literature, there are many of finite element analysis studies that have investigated the skeletal effects with different amounts of maxillary expansion (7, 8, 22, 28-30). In some of these studies, displacement patterns were investigated based on moderate maxillary transverse deficiency after 5 mm expansion as in our study (15). A similar method was followed to allow the comparison of the results.
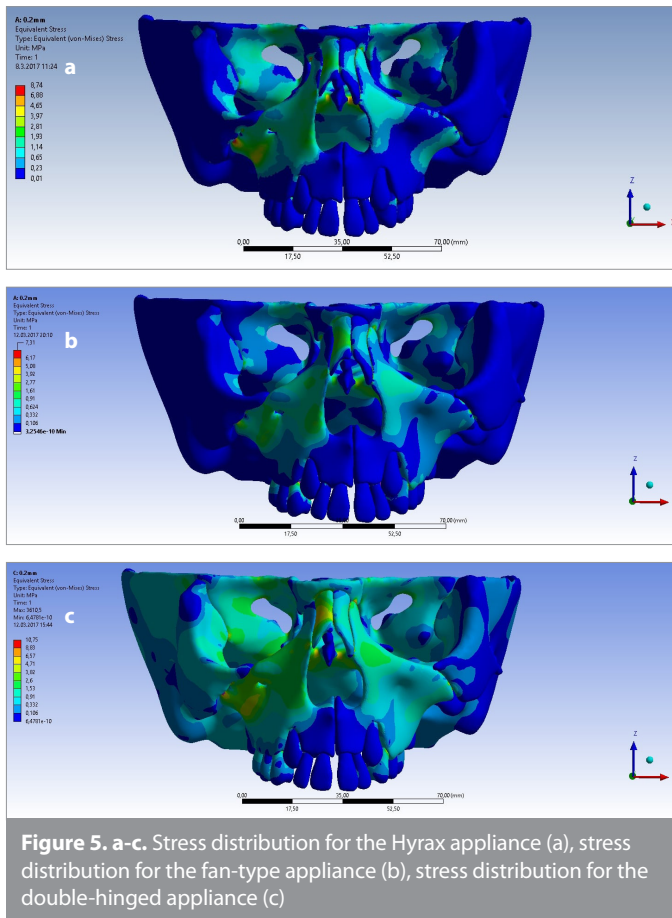
Displacement Pattern in the X-axis
A wedge-shaped opening was observed with all 3 appliances. In the transverse plane, the maximum posterior expansion was achieved with the Hyrax appliance (1.55 mm), whereas the maximum anterior expansion was observed with the double-hinged appliance (2.21 mm).

In the internasal and front maxillary suture area, slight medial displacement was observed with the Hyrax and fan-type appliances, whereas slight lateral displacement was observed with the double-hinged appliance.

The lateral nasal walls showed lateral displacement with all 3 appliances; 0.75 mm, 0.79 mm, and 1.08 mm lateral displacements were observed with the Hyrax, fan-type, and double-hinged appliances, respectively.

The inferior parts of the pterygoid plates showed greater displacements than the superior parts (Tables 2 and 3).

raphy scan images of a 12-year-old male patient with maxillary transverse deficiency, 3D finite element models were generated with institutional review board approval. The parents/legal guard-

Sucu et al. FEM Analysis of Three Different RME Appliances

Turk J Orthod 2021; 34(1): 18-25

Figure 5. a-c. Stress distribution for the Hyrax appliance (a), stress distribution for the fan-type appliance (b), stress distribution for the double-hinged appliance (c)

Displacement Pattern in the Y-axis
The maxilla moved anteriorly with all 3 appliances. The greatest anterior displacement of the maxilla was recorded with the double-hinged appliance (1.44 mm).

The lateral nasal walls showed anterior displacement with all 3 appliances; 0.13 mm, 0.1 mm, and 1.22 mm anterior displacements were observed with the Hyrax, fan-type, and double-hinged appliances, respectively.

The dentoalveolar complex moved posteriorly with the Hyrax appliance (central incisor-0.16 mm), whereas anterior displacement was recorded with the fan-type (central incisor-0.08 mm) and double-hinged appliances (central incisor-0.41 mm) (Tables 2 and 3).

Displacement Pattern in the Z-axis
The maxilla moved inferiorly with all 3 appliances. The greatest inferior displacement of the maxilla was recorded with the Hyrax appliance (1.34 mm).

The maxilla rotated posteriorly with anterior nasal spine (ANS) showing more inferior displacement than posterior nasal spine (PNS) with the Hyrax and fan-type appliances, whereas parallel movement occurred with the double-hinged appliance.

The lateral nasal walls showed inferior displacement with all 3 appliances; 1.04 mm, 0.33 mm, and 0.13 mm inferior displacements

were observed with the Hyrax, fan-type, and double-hinged appliances, respectively.

When all the anatomical structures were evaluated in the vertical plane, greater inferior displacement was recorded with the Hyrax appliance than the fan-type and double-hinged appliances (Tables 2 and 3).

Von Mises Stress Pattern
The stress distribution with the initial 0.2 mm of expansion is presented in a color band, with different colors representing various stress levels, where red indicates areas with the highest stress and blue indicates the lowest stress (Figure 5a, b, and c.)

The highest stress accumulation was observed in the sutura zygomatico maxillaris area (Hyrax=6.39 MPa, fan type=4.32 Mpa, double-hinged=4.46 MPa) with all 3 appliances.

An increase of stress was noted at the pterygomaxillary fissure and medial and lateral pterygoid plates of the sphenoid bone and the nasal areas. When all the anatomical structures were evaluated overall, the stress distributions were found to be the highest with the Hyrax expansion screw, and the lowest values were recorded with the fan-type expansion screw (Tables 4 and 5).

DISCUSSION

Previous orthodontic FEM studies used shell elements for meshing the models (7, 8). However, we used tetrahedral elements with 10 nodes, which have previously been proven to provide better stress transmissibility and bending deformations, for mesh generation (22).

The number of elements that constitute the working model and the number of nodes that each element includes are important factors affecting the sensitivity and reliability of the finite element analysis. In previous studies, Işeri et al. (7) used 2,349 elements and 2,147 nodes; Jafari et al. (8) used 6,951 elements and 7,357 nodes; and Gautam et al. (22) used 108,799 elements and 193,633 nodes. The models used in this study included approximately 1,800,000 volumetric elements and 2,750,000 nodes.

In our study, the wedge-shaped opening was observed with all 3 appliances. In the transverse plane, the maximum posterior expansion was achieved with the Hyrax appliance and the maximum anterior expansion was observed with the double-hinged appliance. Several studies have explained the wedge-shaped opening in the anteroposterior plane as a result of the resistance generated in the pterygomaxillary connection (2, 6). The difference between the opening patterns is thought to be related to the screw design.

The maxilla moved inferiorly and anteriorly with all 3 appliances in the vertical and sagittal planes. The inferior and anterior movement of the maxilla resulting from the RME procedure has been previously reported in many studies (2, 7, 8, 22, 23). Sicher (24) reported that the maxillocranial sutures produce inferior and anterior movement of the maxilla after the RME. Wertz (2)

suggested that separation of the maxillary complex from the pterygoid process could allow significant anterior movement of the maxilla. Gardner and Kronman (23) related the anterior maxillary displacement to the opening of the spheno-occipital synchondrosis. However, Da Silva Filho et al. (25) found no sagittal movement related to the maxilla, but they reported changes in the vertical plane and inferior displacement.

Taking into account the displacement pattern of the maxilla, Dr. Liou (12) designed the double-hinged expansion screw. He stated that the double-hinged appliance provided a greater anterior displacement of the maxilla with less chance of bone resorption behind the maxillary tuberosity. He also stated that the double-hinged appliance significantly displaced the maxilla more anteriorly compared with the Hyrax appliance in an experimental study in 14 cats (13). This finding is similar to that of our study. The highest anterior displacement was observed with the double-hinged screw. We believe that the design of the double-hinged screw moves the center of rotation of the maxilla during opening behind the area of tuberosity, causing the forward movement of the maxilla.

Doruk et al. (10) compared the effects of the Hyrax and fan-type appliances and reported that the maxilla moved inferiorly and anteriorly in both the groups. Their findings showed that the fan-type appliance also forced the maxilla anteriorly more than the Hyrax appliance. The authors argued that the fan-type appliance had a buttressing effect on the skeletal structures behind the maxilla, which explained the rotational opening (10). In this study, the greatest maxillary inferior displacement was recorded with the Hyrax appliance, whereas the anterior maxillary displacement was the greatest with the double-hinged appliance.

The maxilla rotated posteriorly with the Hyrax and fan-type appliances, whereas parallel movement occurred with the double-hinged appliance. Other studies reported varying degrees of anterior or posterior rotation. Işeri et al. (7) and Gautam et al. (8) reported the posterior rotation of the maxilla with RME in contrast with Jafari et al. (22) who found anterior maxillary rotation.

In the nasal area, a slight medial displacement was observed with the Hyrax and fan-type appliances, whereas slight lateral displacement was observed with the double-hinged appliance. Multiple studies have reported medial displacement of the nasal structures after REM (7, 22). Medial displacement of the nasal area might lead to compression of the tissues. This phenomenon explains the frequent dizziness and the pressure and tension in the nasal bridge, under the eyes, and around the cheekbones reported during palatal expansion therapy (4, 22).

The lateral nasal walls were displaced laterally, inferiorly, and anteriorly with all 3 appliances. These findings show similarities with previous reports, and the movement of the lateral nasal walls and inferior movement of the nasal floor could cause a reduction in the airway resistance (4, 7, 8, 22).

With all 3 appliances, the lateral and medial pterygoid plates showed lateral bending; the inferior portion was displaced more

than the superior part, in agreement with the results of previous research (7, 8, 22). This is because the pterygoid plates are more resistant to bending in the parts that are closer to the cranial base (3). Similarly, in our study, lower stress levels were noted for the inferior parts of the plates, and higher stress levels were reported for the superior parts.

Doruk et al. (10) reported that Hyrax caused palatal tipping of the upper incisors, whereas the fan-type appliance caused labial tipping of upper incisors. Similarly, in this study, palatal tipping of the upper incisors was recorded with the Hyrax appliance and labial tipping of upper incisors was recorded with the fan-type and double-hinged appliances (10).

When all the anatomical structures were evaluated in the vertical plane, a tendency toward inferior displacement was recorded with the Hyrax appliance. This is in agreement with the findings of previous studies (2, 25). However, some studies reported that expanded vertical dimensions decrease after the retention phase and the changes that occur are not permanent (26, 27).

Previous studies reported that the main resistance to RME occurred not only in the median palatal suture but also in the sphenoid and zygomatic bones (8, 14).

Işeri et al. (7) observed large amounts of stress accumulation in the canine and molar areas in the maxillary arch, on the lateral sides of the inferior nasal cavity, on the pterygoid plates of the sphenoid bone, and on the zygomatic and nasal bones with RME. Jafari et al. (8) reported that the greatest stress accumulation was seen in the internasal, nasofrontal, and nasomaxillary sutures. Gautam et al. (22) found maximum stress accumulation along the frontomaxillary, nasomaxillary, and frontonasal sutures.

In this study, the maximum stress accumulation was observed in the sutura zygomatico maxillaris area with all 3 appliances. An increase of stress was noted at the pterygomaxillary fissure, medial and lateral pterygoid plates of the sphenoid bone, and the nasal areas. The overall stress distribution values were found to be the highest with the Hyrax expansion screw, and the lowest values were recorded with the fan-type expansion screw.

Similar to the results of our study, Matsuyama et al. (28) found the highest stress levels in the zygomatic process, pterygomaxillary fissure, and tuberous maxilla area with RME. Lee et al. (29) found the highest stress levels in the zygomatico maxillary suture. Mac Ginnis et al. (30) reported high stress levels in the zygomatico maxillary suture, zygomatic process, lateral pterygoid plate, and palatine bone.

Although RME is mainly performed for correcting transversal problems, different vertical and sagittal effects may occur depending on the choice of the appliance. This study aimed to shed light on the selection of the most appropriate expansion appliance according to the skeletal and dental relationship of the patients, either in the vertical or sagittal planes. However, the limitations of the FEM studies, especially the absence of soft tissue, should be considered. Further studies modeling soft tissues

Sucu et al. FEM Analysis of Three Different RME Appliances

Turk J Orthod 2021; 34(1): 18-25

also should be performed to better simulate the clinical scenario. A similar study could be performed *in vivo* with identical triplets presenting with similar maxillary constriction, although it would be difficult to find suitable patients.

Despite all its advantages, it should be noted that finite element analysis is a simulation scenario created by researchers. It requires a computer with sufficient hardware equipped with expensive software that needs regular updates. Another disadvantage is that it requires some presumptions (homogeneous, linear, and isotropic) to simplify the real situation as it is not possible to model all of the complex anatomical structures or to consider all their mechanical properties. There are also other disadvantages, such as the need for detailed information transfer regarding the material properties, loading of the applied forces into the system, and the extensive time required to perform the analysis. In this study, only the initial displacements and stress distributions were studied, which could be considered a limitation considering the dynamic nature of the real clinical application.

CONCLUSION

The following conclusions can be drawn per the results of our study:

1. A wedge-shaped opening was observed, and the maxilla moved inferiorly and anteriorly with all 3 appliances.
2. The maxilla rotated posteriorly with the Hyrax and fan-type appliances, and parallel movement occurred with the double-hinged appliance.
3. The dentoalveolar complex moved posteriorly with the Hyrax appliance, whereas anterior displacement was recorded with the fan-type and double-hinged appliances.
4. The maximum stress was found in the sutura zygomatico maxillaris with all 3 appliances.

Some clinical projections to be considered are the use of fan-type and double-hinged expansion appliances in cases where the maxillary constriction is located more anteriorly. However, the Hyrax appliance may be preferred in patients with excessive posterior constriction. The double-hinged and fan-type appliances seem to be more advantageous for providing vertical control compared with the Hyrax appliance and thus should be preferred in patients with increased vertical height. Considering the displacement of the dental structures, it might be hypothesized that the Hyrax appliance could play an auxiliary role in camouflage treatment of dental Class II malocclusion and the double-hinged appliance in the treatment of the dental Class III malocclusion. Nevertheless, these suggestions need to be justified with further clinical studies.

REFERENCES

1. McNamara JA, Brudon WL, Kokich VG. Orthodontics and dentofacial orthopedics 2001: Needham Press.
2. Wertz RA. Skeletal and dental changes accompanying rapid midpalatal suture opening. Am J Orthod Dentofacial Orthop 970; 58: 41-66. [Crossref]
3. Timms DJ. A study of basal movement with rapid maxillary expansion. Am J Orthod Dentofacial Orthop 1980; 77: 500-7. [Crossref]
4. Haas AJ. The treatment of maxillary deficiency by opening the midpalatal suture. Angle Orthod 1965; 35: 200-17.
5. Starnbach H, Bayne D, Cleall J, Subtelny JD. Facioskeletal And Dental Changes Resulting From Rapid Maxillary Expansion. Angle Orthod 1966; 36: 152-64.
6. Isaacson R, Wood J, Ingram A. Forces produced by rapid maxillary expansion. Part I. Design of the force measuring system. Angle Orthod 1964; 34: 256-60.
7. Işeri H, Tekkaya AE, Öztan Ö, Bilgic S. Biomechanical effects of rapid maxillary expansion on the craniofacial skeleton, studied by the finite element method. Eur J Orthod 1998; 20: 347-56. [Crossref]
8. Jafari A, Shetty KS, Kumar M. Study of stress distribution and displacement of various craniofacial structures following application of transverse orthopedic forces-a three-dimensional FEM study. Angle Orthod 2003; 73: 12-20.
9. de Sousa Araugio RM, Landre Jr J, Silva DDLA, Pacheco W, Pithon MM, Oliveira DD. Influence of the expansion screw height on the dental effects of the hyrax expander: a study with finite elements. Am J Orthod Dentofacial Orthop 2013; 143: 221-7. [Crossref]
10. Doruk C, Bicakci AA, Basciftci FA, Agar U, Babacan H. A comparison of the effects of rapid maxillary expansion and fan-type rapid maxillary expansion on dentofacial structures. Angle Orthod 2004; 74: 184-94.
11. Çörekçi B, Göyenç YB. Dentofacial changes from fan-type rapid maxillary expansion vs traditional rapid maxillary expansion in early mixed dentition: A prospective clinical trial. Angle Orthod 2013; 83: 842-50. [Crossref]
12. Huang C, Wang Y, Huang C, Liou E. Maxillary displacement after rapid maxillary expansions: An animal study. J. Taiwan Assoc. Orthod Taipei 2008; 20: 19-31.
13. EJ. L. Interview. Rev Dent Press Orthodon Ortop Facial. 2009; 14.
14. Bishara SE, Staley RN. Maxillary expansion: clinical implications. Am J Orthod Dentofacial Orthop 1987; 91: 3-14. [Crossref]
15. Lee H, Nguyen A, Hong C, Hoang P, Pham J, Ting K. Biomechanical effects of maxillary expansion on a patient with cleft palate: A finite element analysis. Am J Orthod Dentofacial Orthop 2016; 150: 313-23. [Crossref]
16. Ludwig B, Baumgaertel S, Zorkun B, Bonitz L, Glasl B, Wilmes B, et al. Application of a new viscoelastic finite element method model and analysis of miniscrew-supported hybrid hyrax treatment. Am J Orthod Dentofacial Orthop 2013; 143: 426-35. [Crossref]

Turk J Orthod 2021; 34(1): 18-25

Sucu et al. FEM Analysis of Three Different RME Appliances

17. Tanne K, Yoshida S, Kawata T, Sasaki A, Knox J, Jones ML. An evaluation of the biomechanical response of the tooth and periodontium to orthodontic forces in adolescent and adult subjects. British Journal of Orthodontics 1998; 25: 109-15. [Crossref]

18. Gupta A, Kohli VS, Hazarey PV, Kharbanda OP, Gunjal A. Stress distribution in the temporomandibular joint after mandibular protraction: a 3-dimensional finite element method study. Part 1. Am J Orthod Dentofacial Orthop 2009; 135: 737-48. [Crossref]

19. Vásquez M, Calao E, Becerra F, Ossa J, Enríquez C, Fresneda E. Initial stress differences between sliding and sectional mechanics with an endosseous implant as anchorage: a 3-dimensional finite element analysis. Angle Orthod 2001; 71: 247-56.

20. Henderson JH, Longaker MT, Carter DR. Sutural bone deposition rate and strain magnitude during cranial development. Bone 2004; 34: 271-80. [Crossref]

21. Lee H, Tin K, Nelson M, Sun N, Sung SJ. Maxillary expansion in customized finite element method models. Am J Orthod Dentofacial Orthop 2009; 136: 367-74. [Crossref]

22. Gautam P, Valiathan A, Adhikari R. Stress and displacement patterns in the craniofacial skeleton with rapid maxillary expansion: a finite element method study. Am J Orthod Dentofacial Orthop 2007; 132: 5. e1-5. e11. [Crossref]

23. Gardner GE, Kronman JH. Cranioskeletal displacements caused by rapid palatal expansion in the rhesus monkey. Am J Orthod Dentofacial Orthop 1971; 59: 146-55. [Crossref]

24. Sicher H. Oral anatomy. 1965: CV Mosby Company.

25. de Silva Fo OG, Boas CV, Capelozza LF. Rapid maxillary expansion in the primary and mixed dentitions: a cephalometric evaluation. Am J Orthod Dentofacial Orthop 1991; 100: 171-9. [Crossref]

26. Velázquez P, Benito E, Bravo LA. Rapid maxillary expansion. A study of the long-term effects. Am J Orthod Dentofacial Orthop 1996; 109: 361-7. [Crossref]

27. Lagravere MO, Major PW, Flores-Mir C. Skeletal and dental changes with fixed slow maxillary expansion treatment: a systematic review. J Am Dent Assoc 2005; 136: 194-9. [Crossref]

28. Matsuyama Y, Motoyoshi M, Tsurumachi N, Shimizu N. Effects of palate depth, modified arm shape, and anchor screw on rapid maxillary expansion: a finite element analysis. Eur J Orthod 2015: 188-93. [Crossref]

29. Lee SC, Park JH, Bayome M, Kim KB, Araujo EA, Kook YA. Effect of bone-borne rapid maxillary expanders with and without surgical assistance on the craniofacial structures using finite element analysis. Am J Orthod Dentofacial Orthop 2014; 145: 638-48. [Crossref]

30. MacGinnis M, Chu H, Youssef G, Wu KW, Machado AW, Moon W. The effects of micro-implant assisted rapid palatal expansion (marpe) on the nasomaxillary complex-a finite element method (FEM) analysis. Prog Orthod 2014; 15: 52. [Crossref]